

Deep Learning for Detecting Multiple Space-Time Action Tubes in Videos

Suman Saha¹

suman.saha-2014@brookes.ac.uk

Gurkirt Singh¹

gurkirt.singh-2015@brookes.ac.uk

Michael Sapienza²

michael.sapienza@eng.ox.ac.uk

Philip H. S. Torr²

philip.torr@eng.ox.ac.uk

Fabio Cuzzolin¹

fabio.cuzzolin@brookes.ac.uk

¹ Dept. of Computing and
Communication Technologies
Oxford Brookes University
Oxford, UK

² Department of Engineering Science
University of Oxford
Oxford, UK

Abstract

In this work, we propose an approach to the spatiotemporal localisation (detection) and classification of multiple concurrent actions within temporally untrimmed videos. Our framework is composed of three stages. In stage 1, appearance and motion detection networks are employed to localise and score actions from colour images and optical flow. In stage 2, the appearance network detections are boosted by combining them with the motion detection scores, in proportion to their respective spatial overlap. In stage 3, sequences of detection boxes most likely to be associated with a single action instance, called action tubes, are constructed by solving two energy maximisation problems via dynamic programming. While in the first pass, action paths spanning the whole video are built by linking detection boxes over time using their class-specific scores and their spatial overlap, in the second pass, temporal trimming is performed by ensuring label consistency for all constituting detection boxes. We demonstrate the performance of our algorithm on the challenging UCF101, J-HMDB-21 and LIRIS-HARL datasets, achieving new state-of-the-art results across the board and significantly increasing detection speed at test time.

1 Introduction

Recent advances in object detection via convolutional neural networks (CNNs) [7] have triggered a significant performance improvement in the state-of-the-art action detectors [8, 34]. However, the accuracy of these approaches is limited by their relying on unsupervised region proposal algorithms such as Selective Search [8] or EdgeBoxes [34] which, besides being resource-demanding, cannot be trained for a specific detection task and are disconnected from the overall classification objective. Moreover, these approaches are computationally expensive as they follow a multi-stage classification strategy which requires CNN fine-tuning and intensive feature extraction (at both training and test time), the caching of these features

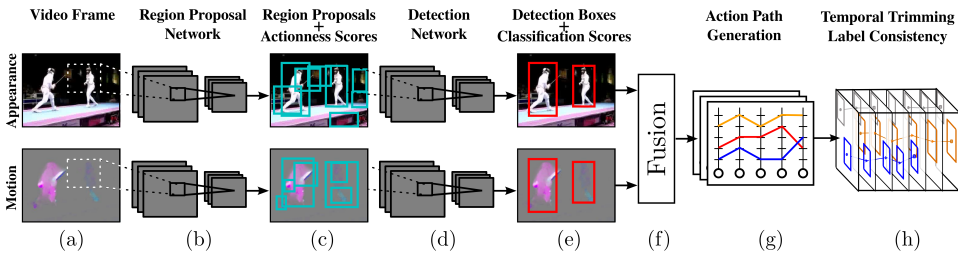


Figure 1: At test time, (a) RGB and optical-flow images are passed to (b) two separate region proposal networks (RPNs). (c) Each network outputs region proposals with associated actionness scores (§ 3.1). (d) Each appearance/motion detection network takes as input the relevant image and RPN-generated region proposals, and (e) outputs detection boxes and softmax probability scores (§ 3.2). (f) Appearance and motion based detections are fused (§ 3.3) and (g) linked up to generate class-specific action paths spanning the whole video. (h) Finally the action paths are temporally trimmed to form action tubes (§ 3.4).

onto disk, and finally the training of a battery of one-vs-all SVMs for action classification. On large datasets such as UCF-101 [25], overall training and feature extraction takes a week using 7 Nvidia Titan X GPUs, plus one extra day for SVM training. At test time, detection is slow as features need to be extracted for each region proposal via a CNN forward pass.

To overcome these issues we propose a novel action detection framework which, instead of adopting an expensive multi-stage pipeline, takes advantage of the most recent single-stage deep learning architectures for object detection [21], in which a single CNN is trained for both detecting and classifying frame-level region proposals in an end-to-end fashion. Detected frame-level proposals are subsequently linked in time to form space-time ‘action tubes’ [8] by solving two optimisation problems via dynamic programming. We demonstrate that the proposed action detection pipeline is at least $2\times$ faster in training and $5\times$ faster in test time detection speeds as compared to [8, 34]. In the supplementary material, we present a comparative analysis of the training and testing time requirements of our approach with respect to [8, 34] on the UCF-101 [25] and J-HMDB-21 [12] datasets. Moreover, our pipeline consistently outperforms previous state-of-the-art results (§ 4).

Overview of the approach. Our approach is summarised in Fig. 1. We train two pairs of Region Proposal Networks (RPN) [21] and Fast R-CNN [6] detection networks - one on RGB and another on optical-flow images [8]. For each pipeline, the RPN (b), takes as input a video frame (a), and generates a set of region proposals (c), and their associated ‘actionness’ [2] scores¹. Next, a Fast R-CNN [21] detection network (d) takes as input the original video frame and a subset of the region proposals generated by the RPN, and outputs a ‘regressed’ detection box and a softmax classification score for each input proposal, indicating the probability of an action class being present within the box. To merge appearance and motion cues, we fuse (f) the softmax scores from the appearance- and motion-based detection boxes (e) (§ 3.3). We found that this strategy significantly boosts detection accuracy.

After fusing the set of detections over the entire video, we identify sequences of frame regions most likely to be associated with a single action tube. Detection boxes in a tube need to display a high score for the considered action class, as well as a significant spatial overlap for consecutive detections. Class-specific action paths (g) spanning the whole video duration are generated via a Viterbi forward-backward pass (as in [8]). An additional second pass of

¹A softmax score for a region proposal containing an action or not.

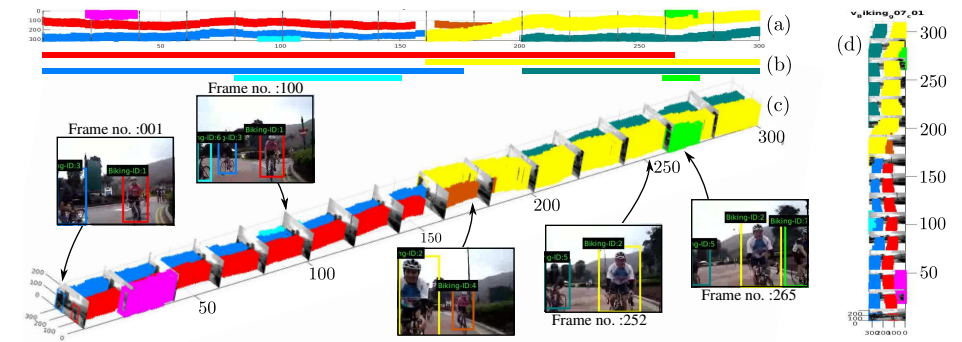


Figure 2: Action tube detection in a ‘biking’ video taken from UCF-101 [25]. (a) Side view of the detected action tubes where each colour represents a particular instance. The detection boxes in each frame are linked up to form space-time action tubes. (b) Illustration of the ground-truth temporal duration for comparison. (c) Viewing the video as a 3D volume with selected image frames; notice that we are able to detect multiple action instances in both space and time. (d) Top-down view.

dynamic programming is introduced to take care of temporal detection (h). As a result, our action tubes are not constrained to span the entire video duration, as in [8]. Furthermore, extracting multiple paths allows our algorithm to account for multiple co-occurring instances of the same action class (see Fig. 2).

Although it makes use of existing RPN [21] and Fast R-CNN [6] architectures, this work proposes a radically new approach to spatiotemporal action detection which brings them together with a novel late fusion approach and an original action tube generation mechanism to dramatically improve accuracy and detection speed. Unlike [8, 34], in which appearance and motion information are fused by combining fc7 features, we follow a late fusion approach [23]. Our novel fusion strategy boosts the confidence scores of the detection boxes based on their spatial overlaps and their class-specific softmax scores obtained from appearance and motion based networks (§ 3.3). The 2nd pass of dynamic programming, we introduce for action tube temporal trimming, contributes to a great extent to significantly improve the detection performance (§ 4).

Contributions. In summary, this work’s main contribution is a novel action detection pipeline which:

- incorporates recent deep Convolutional Neural Network architectures for simultaneously predicting frame-level detection boxes and the associated action class scores (§ 3.1-3.2);
- uses an original fusion strategy for merging appearance and motion cues based on the softmax probability scores and spatial overlaps of the detection bounding boxes (§ 3.3);
- brings forward a two-pass dynamic programming (DP) approach for constructing space time action tubes (§ 3.4).

An extensive evaluation on the main action detection datasets demonstrates that our approach significantly outperforms the current state-of-the-art, and is 5 to 10 times faster than the main competitors at detecting actions at test time (§ 4). Thanks to our two-pass action tube generation algorithm, in contrast to most existing action classification [13, 15, 23, 30, 31] and localisation [8, 34] approaches, our method is capable of detecting and localising multiple co-occurring action instances in temporally untrimmed videos (see Fig. 2).

2 Related work

Recently, inspired by the record-breaking performance of CNNs in image classification [17] and object detection from images [7], deep learning architectures have been increasingly applied to action classification [13, 15, 23], spatial [8] or spatio-temporal [34] action localisation, and event detection [37].

The action localisation problem, in particular, can be addressed by leveraging video segmentation methods. An example is the unsupervised greedy agglomerative clustering approach of [11], which resembles Selective Search space-time video blocks. Since [11] does not exploit the representative power of CNN features, they fail to achieve state-of-the-art results. Soomro *et al.* [26] learn the contextual relations between different space-time video segments. Such ‘supervoxels’, however, may end up spanning very long time intervals, failing to localise each action instance individually. Similarly, [29] uses unsupervised clustering to generate a small set of bounding box-like spatio-temporal action proposals. However, since the approach in [29] employs dense-trajectory features [30], it does not work on actions characterised by small motions [29].

The temporal detection of actions [9, 14] and gestures [3] in temporally untrimmed videos has also recently attracted much interest [4, 38]. Sliding window approaches have been extensively used [5, 19, 27, 32]. Unlike our approach, these methods [27, 32, 38] only address *temporal* detection, and suffer from the inefficient nature of temporal sliding windows. Our framework is based on incrementally linking frame-level region proposals and temporal smoothing (in a similar fashion to [4]), an approach which is computationally more efficient and can handle long untrimmed videos.

Indeed methods which connect frame-level region proposals for joint spatial and temporal localisation have risen to the forefront of current research. Gkioxari and Malik [8] have extended [7] and [23] to tackle action detection using unsupervised Selective-Search region proposals and separately trained SVMs. However, as the videos used to evaluate their work only contain one action and were already temporally trimmed (J-HMDB-21 [12]), it is not possible to assess their temporal localisation performance. Weinzaepfel *et al.*’s approach [34], instead, first generates region proposals using EdgeBoxes [40] at frame level to later use a tracking-by-detection approach based on a novel track-level descriptor called a Spatio-Temporal Motion Histogram. Moreover, [34] achieves temporal trimming using a multi-scale sliding window over each track, making it inefficient for longer video sequences. Our approach improves on both [8, 34] by using an efficient two-stage single network for detection of region proposals and two passes of dynamic programming for tube construction.

Some of the reviewed approaches [29, 34] could potentially be able to detect co-occurring actions. However, [34] limit their method to produce maximum of two detections per class, while [29] does so on the MSRII dataset [1] which only contains three action classes of repetitive nature (clapping, boxing and waving). Klaser *et al.* [16] use a space-time descriptor and a sliding window classifier to detect the location of only two actions (phoning and standing up). In contrast, in our LIRIS-HARL tests (§ 4) we consider 10 diverse action categories.

3 Methodology

As outlined in Figure 1, our approach combines a region-proposal network (§ 3.1-Fig. 1b) with a detection network (§ 3.2-Fig. 1d), and fuses the outputs (§ 3.3-Fig. 1f) to generate action tubes (§ 3.4-Fig. 1g-h). All components are described in detail below.

3.1 Region Proposal Network

To generate rectangular action region hypotheses in a video frame we adopt the Region Proposal Network (RPN) approach of [21], which is built on top of the last convolutional layer of the VGG-16 architecture by Simonyan and Zisserman [24]. To generate region proposals, this mini-network slides over the convolutional feature map outputted by the last layer, processing at each location an $n \times n$ spatial window and mapping it to a lower dimensional feature vector (512-d for VGG-16). The feature vector is then passed to two fully connected layers: a box-regression layer and a box-classification layer.

During training, for each image location, k region proposals (also called ‘anchors’) [21] are generated. We consider those anchors with a high Intersection-over-Union (IoU) with the ground-truth boxes ($IoU > 0.7$) as positive examples, whilst those with $IoU < 0.3$ as negatives. Based on these training examples, the network’s objective function is minimised using stochastic gradient descent (SGD), encouraging the prediction of both the probability of an anchor belonging to action or no-action category (a binary classification), and the 4 coordinates of the bounding box.

3.2 Detection network

For the detection network we use a Fast R-CNN net [6] with a VGG-16 architecture [24]. This takes the RPN-based region proposals (§ 3.1) and regresses a new set of bounding boxes for each action class and associates classification scores. Each RPN-generated region proposal leads to C (number of classes) regressed bounding boxes with corresponding class scores.

Analogously to the RPN component, the detection network is also built upon the convolutional feature map outputted by the last layer of the VGG-16 network. It generates a feature vector for each proposal generated by RPN, which is again fed to two sibling fully-connected layers: a box-regression layer and a box-classification layer. Unlike what happens in RPNs, these layers produce C multi-class softmax scores and refined boxes (one for each action category) for each input region proposal.

CNN training strategy. We employ a variation on the training strategy of [21] to train both the RPN and Fast R-CNN networks. Shaoqing *et al.* [21] suggested a 4-steps ‘alternating training’ algorithm in which in the first 2 steps, a RPN and a Fast R-CNN nets are trained independently, while in the 3rd and 4th steps the two networks are fine-tuned with shared convolutional layers. In practice, we found empirically that the detection accuracy on UCF101 slightly decreases when using shared convolutional features, i.e., when fine tuning the RPN and Fast-RCNN trained models obtained after the first two steps. As a result, we train the RPN and the Fast R-CNN networks independently following only the 1st and 2nd steps of [21], while neglecting the 3rd and 4th steps suggested by [21].

3.3 Fusion of appearance and motion cues

In a work by Redmon *et al.* [20], the authors combine the outputs from Fast R-CNN and YOLO (You Only Look Once) object detection networks to reduce background detections and improve the overall detection quality. Inspired by their work, we use our motion-based detection network to improve the scores of the appearance-based detection net (c.f. Fig. 1f).

Let $\{\mathbf{b}_i^s\}$ and $\{\mathbf{b}_i^f\}$ denote the sets of detection boxes generated by the appearance- and motion-based detection networks, respectively, on a given test frame and for a specific action

class c . Let \mathbf{b}_{max}^f be the motion-based detection box with maximum overlap with a given appearance-based detection box \mathbf{b}_i^s . If this maximum overlap, quantified using the IoU, is above a given threshold τ , we augment the softmax score $s_c(\mathbf{b}_i^s)$ of the appearance-based box as follows:

$$s_c^*(\mathbf{b}_i^s) = s_c(\mathbf{b}_i^s) + s_c(\mathbf{b}_{max}^f) \times IoU(\mathbf{b}_i^s, \mathbf{b}_{max}^f). \quad (1)$$

The second term adds to the existing score of the appearance-based detection box a proportion, equal to the amount of overlap, of the motion-based detection score. In our tests we set $\tau = 0.3$.

3.4 Action tube generation

The output of our fusion stage (§ 3.3) is, for each video frame, a collection of detection boxes for each action category, together with their associated augmented classification scores (1). Detection boxes can then be linked up in time to identify video regions most likely to be associated with a single action instance, or *action tube*. Action tubes are connected sequences of detection boxes in time, without interruptions, and unlike those in [8] they are not constrained to span the entire video duration.

They are obtained as solutions to two consecutive energy maximisation problems. First a number of action-specific paths $\mathbf{p}_c = \{\mathbf{b}_1, \dots, \mathbf{b}_T\}$, spanning the entire video length, are constructed by linking detection boxes over time in virtue of their class-specific scores and their temporal overlap. Second, action paths are temporally trimmed by ensuring that the constituting boxes' detection scores are consistent with the foreground label c .

Building action paths. We define the energy $E(\mathbf{p}_c)$ for a particular path \mathbf{p}_c linking up detection boxes for class c across time to be the a sum of unary and pairwise potentials:

$$E(\mathbf{p}_c) = \sum_{t=1}^T s_c^*(\mathbf{b}_t) + \lambda_o \sum_{t=2}^T \psi_o(\mathbf{b}_t, \mathbf{b}_{t-1}), \quad (2)$$

where $s_c^*(\mathbf{b}_t)$ denotes the augmented score (1) of detection \mathbf{b}_t , the overlap potential $\psi_o(\mathbf{b}_t, \mathbf{b}_{t-1})$ is the IoU of the two boxes \mathbf{b}_t and \mathbf{b}_{t-1} , and λ_o is a scalar parameter weighting the relative importance of the pairwise term. The value of the energy (2) is high for paths whose detection boxes score highly for the particular action category c , and for which consecutive detection boxes overlap significantly. We can find the path which maximises the energy, $\mathbf{p}_c^* = \operatorname{argmax}_{\mathbf{p}_c} E(\mathbf{p}_c)$, by simply applying the Viterbi algorithm [8].

Once an optimal path has been found, we remove all the detection boxes associated with it and recursively seek the next best action path. Extracting multiple paths allows our algorithm to account for multiple co-occurring instances of the same action class.

Smooth path labelling and temporal trimming. As the resulting action-specific paths span the entire video duration, while human actions typically only occupy a fraction of it, temporal trimming becomes necessary. The first pass of dynamic programming (2) aims at extracting connected paths by penalising regions which do not overlap in time. As a result, however, not all detection boxes within a path exhibit strong action-class scores.

The goal here is to assign to every box $\mathbf{b}_t \in \mathbf{p}_c$ in an action path \mathbf{p}_c a binary label $l_t \in \{c, 0\}$ (where zero represents the 'background' or 'no-action' class), subject to the conditions that the path's labelling $\mathbf{L}_{\mathbf{p}_c} = [l_1, l_2, \dots, l_T]'$: i) is consistent with the unary scores (1);

and ii) is smooth (no sudden jumps).

As in the previous pass, we may solve for the best labelling by maximising:

$$\mathbf{L}_{\mathbf{p}_c}^* = \underset{\mathbf{L}_{\mathbf{p}_c}}{\operatorname{argmax}} \left(\sum_{t=1}^T s_{l_t}(\mathbf{b}_t) - \lambda_l \sum_{t=2}^T \psi_l(l_t, l_{t-1}) \right), \quad (3)$$

where λ_l is a scalar parameter weighting the relative importance of the pairwise term. The pairwise potential ψ_l is defined to be:

$$\psi_l(l_t, l_{t-1}) = \begin{cases} 0 & \text{if } l_t = l_{t-1} \\ \alpha_c & \text{otherwise,} \end{cases} \quad (4)$$

where α_c is a class-specific constant parameter which we set by cross validation. In the supplementary material, we show the impact of the class-specific α_c on the detection accuracy. Equation (4) is the standard Potts model which penalises labellings that are not smooth, thus enforcing a piecewise constant solution. Again, we solve (3) using the Viterbi algorithm.

All contiguous subsequences of the retained action paths \mathbf{p}_c associated with category label c constitute our action tubes. As a result, one or more distinct action tubes spanning arbitrary temporal intervals may be found in each video for each action class c . Finally, each action tube is assigned a global score equal to the mean of the top k augmented class scores (1) of its constituting detection boxes.

4 Experimental validation and discussion

In order to evaluate our spatio-temporal action detection pipeline we selected what are currently considered among the most challenging action detection datasets: UCF-101 [25], LIRIS HARL D2 [36], and J-HMDB-21 [12]. UCF-101 is the largest, most diverse and challenging dataset to date, and contains realistic sequences with a large variation in camera motion, appearance, human pose, scale, viewpoint, clutter and illumination conditions. Although each video only contains a single action category, it may contain multiple action instances of the same action class. To achieve a broader comparison with the state-of-the-art, we also ran tests on the J-HMDB-21 [12] dataset. The latter is a subset of HMDB-51 [18] with 21 action categories and 928 videos, each containing a single action instance and trimmed to the action’s duration. The reported results were averaged over the three splits of J-HMDB-21. Finally we conducted experiments on the more challenging LIRIS-HARL dataset, which contains 10 action categories, including human-human interactions and human-object interactions (e.g., ‘discussion of two or several people’, and ‘a person types on a keyboard’²). In addition to containing multiple space-time actions, some of which occurring concurrently, the dataset contains scenes where relevant human actions take place amidst other irrelevant human motion.

For all datasets we used the exact same evaluation metrics and data splits as in the original papers. In the supplementary material, we further discuss all implementation details, and propose an interesting quantitative comparison between Selective Search- and RPN-generated region proposals.

Performance comparison on UCF-101. Table 1 presents the results we obtained on UCF-101, and compares them to the previous state-of-the-art [34, 39]. We achieve an mAP of

²<http://liris.cnrs.fr/voir/activities-dataset>

Table 1: Quantitative action detection results (mAP) on the UCF-101 dataset.

Spatio-temporal overlap threshold δ	0.05	0.1	0.2	0.3	0.4	0.5	0.6
FAP [39]	42.80	—	—	—	—	—	—
STMH [34]	54.28	51.68	46.77	37.82	—	—	—
Our (appearance detection model)	68.74	66.13	56.91	48.28	39.10	30.67	22.77
Our (motion detection model)	67.04	64.86	57.33	47.45	38.65	28.90	19.49
Our (appearance + motion fusion)	79.12	76.57	66.75	55.46	46.35	35.86	26.79

66.75% compared to 46.77% reported by [34] (a 20% gain), at the standard threshold of $\delta = 0.2$. At a threshold of $\delta = 0.4$ we still get a high score of 46.35%, (comparable to 46.77% [34] at $\delta = 0.2$). Note that we are the first to report results on UCF-101 up to $\delta = .6$, attesting to the robustness of our approach to more accurate localisation requirements. Although our separate appearance- and motion-based detection pipelines already outperform the state-of-the-art (Table 1), their combination (§ 3.3) delivers a significant performance increase.

Some representative example results from UCF-101 are shown in Fig. 3. Our method can detect several (more than 2) action instances concurrently, as shown in Fig. 2, in which three concurrent instances and in total six action instances are detected correctly. Quantitatively, we report class-specific video AP (average precision in %) of 88.0, 83.0 and 62.5 on the UCF-101 action categories ‘Fencing’, ‘SalsaSpin’ and ‘IceDancing’, respectively, which all concern multiple inherently co-occurring action instances. Class-specific video APs on UCF-101 are reported in the supplementary material.

Performance comparison on J-HMDB-21. The results we obtained on J-HMDB-21 are presented in Table 2. Our method again outperforms the state-of-the-art, with an mAP increase of 18% and 11% at $\delta = .5$ as compared to [8] and [34], respectively. Note that our motion-based detection pipeline alone exhibits superior results, and when combined with appearance-based detections leads to a further improvement of 4% at $\delta = .5$. These results attest to the high precision of the detections - a large portion of the detection boxes have high IoU overlap with the ground-truth boxes, a feature due to the superior quality of RPN-based region proposals as opposed to Selective Search’s (a direct comparison is provided in the supplementary material). Sample detections on J-HMDB-21 are shown in Figure 4. Also, we list our classification accuracy results on J-HMDB-21 in Table 3, where it can be seen that our method achieves an 8% gain compared to [8].



Figure 3: Action detection/localisation results on UCF101. Ground-truth boxes are in green, detection boxes in red. The top row shows correct detections, the bottom one contains examples of more mixed results. In the last frame, 3 out of 4 ‘Fencing’ instances are nevertheless correctly detected.



Figure 4: Sample space-time action localisation results on JHMDB. Left-most three frames: accurate detection examples. Right-most three frames: mis-detection examples.

Table 2: Quantitative action detection results (mAP) on the J-HMDB-21 dataset.

Spatio-temporal overlap threshold δ	0.1	0.2	0.3	0.4	0.5	0.6	0.7
ActionTube [8] (mAP)	—	—	—	—	53.3	—	—
Wang et al. [33] (mAP)	—	—	—	—	56.4	—	—
STMH [34] (mAP)	—	63.1	63.5	62.2	60.7	—	—
Our (appearance detection model) (mAP)	52.99	52.94	52.57	52.22	51.34	49.55	45.65
Our (motion detection model) (mAP)	69.63	69.59	69.49	69.00	67.90	65.25	54.35
Our (appearance+motion fusion) (mAP)	72.65	72.63	72.59	72.24	71.50	68.73	56.57

Table 3: Classification accuracy on the J-HMDB-21 dataset.

Method	Wang et al. [30]	STMH [34]	ActionTube [8]	Our (appearance+motion fusion)
Accuracy (%)	56.6	61	62.5	70.0

Performance comparison on LIRIS-HARL. LIRIS HARL allows us to demonstrate the efficacy of our approach on temporally un-trimmed videos with co-occurring actions. For this purpose we use LIRIS-HARL’s specific evaluation tool - the results are shown in Table 4. Our results are compared with those of i) VPULABUAM-13 [22] and ii) IACAS-51 [10] from the original LIRIS HARL detection challenge. In this case, our method outperforms the competitors by an even larger margin. We report space-time detection results by fixing the threshold quality level to 10% for the four thresholds [35] and measuring temporal precision and recall along with spatial precision and recall, to produce an integrated score. We refer the readers to [35] for more details on LIRIS HARL’s evaluation metrics.



Figure 5: Frames from the space-time action detection results on LIRIS-HARL, some of which include single actions involving more than one person like ‘handshaking’ and ‘discussion’. Left-most three frames: accurate detection examples. Right-most three frames: mis-detection examples.

We also report in Table 5 the mAP scores obtained by the appearance, motion and the fusion detection models, respectively (note that there is no prior state of the art to report in this case). Again, we can observe an improvement of 7% mAP at $\delta = .2$ due to our fusion strategy. To demonstrate the advantage of our 2nd pass of DP (§ 3.4), we also generate results (mAP) using only the first DP pass (§ 3.4). Without the 2nd pass performance decreases by 20%, highlighting the importance of temporal trimming in the construction of action tubes.

Table 4: Quantitative action detection results on the LIRIS-HARL dataset.

Method	Recall-10	Precision-10	F1-Score-10	I_{sr}	I_{sp}	I_{tr}	I_{tp}	IQ
VPULABUAM-13-IQ [22]	0.04	0.08	0.05	0.02	0.03	0.03	0.03	0.03
IACAS-51-IQ [10]	0.03	0.04	0.03	0.01	0.01	0.03	0.00	0.02
(Ours)	0.568	0.595	0.581	0.5383	0.3402	0.4802	0.4739	0.458

Table 5: Quantitative action detection results (mAP) on LIRIS-HARL for different δ .

Spatio-temporal overlap threshold δ	0.1	0.2	0.3	0.4	0.5
Appearance detection model	46.21	41.94	31.38	25.22	20.43
Motion detection model	52.76	46.58	35.54	26.11	19.28
Appearance+motion fusion with one DP pass	38.1	29.46	23.58	14.54	9.59
Appearance+motion fusion with two DP passes	54.18	49.10	35.91	28.03	21.36

Test-time detection speed comparison. Finally, we compared detection speed at test time of the combined region proposal generation and CNN feature extraction approach used in ([8, 34]) to our neural-net based, single stage action proposal and classification pipeline on the J-HMDB-21 dataset. We found our method to be $10\times$ faster than [8] and $5\times$ faster than [34], with a mean of 113.52 [8], 52.23 [34] and 10.89 (ours) seconds per video, averaged over all the videos in J-HMDB-21 split1. More timing comparison details and qualitative results (images and video clips) can be found in the supplementary material.

Discussion. The superior performance of the proposed method is due to a number of reasons. 1) Instead of using unsupervised region proposal algorithms as in [28, 40], our pipeline takes advantage of a supervised RPN-based region proposal approach which exhibits better recall values than [28] (supplementary-material). 2) Our fusion technique improves the mAPs (over the individual appearance or motion models) by 9.4%, 3.6% and 2.5% on the UCF-101, J-HMDB-21 and LIRIS HARL datasets respectively. We are the first to report an ablation study (supplementary-material) where it is shown that the proposed fusion strategy (§ 3.3) improves the class-specific video APs of UCF-101 action classes. 3) Our original 2nd pass of DP is responsible for significant improvements in mAP by 20% on LIRIS HARL and 6% on UCF-101 (supplementary-material). Additional qualitative results are provided in the supplementary video³, and on the project web page⁴, where the code has also been made available.

5 Conclusions and future work

In this paper, we presented a novel human action recognition approach which addresses in a coherent framework the challenges involved in concurrent multiple human action recognition, spatial localisation and temporal detection, thanks to a novel deep learning strategy for simultaneous detection and classification of region proposals and an improved action tube generation approach. Our method significantly outperforms the previous state-of-the-art on the most challenging benchmark datasets, for it is capable of handling multiple concurrent action instances and temporally untrimmed videos.

Its combination of high accuracy and fast detection speed at test time is very promising for real-time applications, for instance smart car navigation. As the next step we plan to make our tube generation and labelling algorithm fully incremental and online, by only using region proposals from independent frames at test time and updating the dynamic programming optimisation step at every incoming frame.

Acknowledgements. This work was partly supported by ERC grant ERC-2012-AdG 321162-HELIOS, EPSRC grant Seebibyte EP/M013774/1 and EPSRC/MURI grant EP/N019474/1.

³<https://www.youtube.com/embed/vBZsTgjhWaq>

⁴<http://sahasuman.bitbucket.org/bmvc2016>

References

- [1] Liangliang Cao, Zicheng Liu, and Thomas S Huang. Cross-dataset action detection. In *Computer vision and pattern recognition (CVPR), 2010 IEEE conference on*, pages 1998–2005. IEEE, 2010.
- [2] Wei Chen, Caiming Xiong, Ran Xu, and Jason Corso. Actionness ranking with lattice conditional ordinal random fields. In *Proceedings of the IEEE Conference on Computer Vision and Pattern Recognition*, pages 748–755, 2014.
- [3] Sergio Escalera, Xavier Baró, Jordi Gonzalez, Miguel A Bautista, Meysam Madadi, Miguel Reyes, Víctor Ponce-López, Hugo J Escalante, Jamie Shotton, and Isabelle Guyon. Chalearn looking at people challenge 2014: Dataset and results. In *Computer Vision-ECCV 2014 Workshops*, pages 459–473. Springer, 2014.
- [4] G. Evangelidis, G. Singh, and R. Horaud. Continuous gesture recognition from articulated poses. In *ECCV Workshops*, 2014.
- [5] Adrien Gaidon, Zaid Harchaoui, and Cordelia Schmid. Temporal localization of actions with actoms. *Pattern Analysis and Machine Intelligence, IEEE Transactions on*, 35(11):2782–2795, 2013.
- [6] Ross Girshick. Fast R-CNN. In *Proceedings of the IEEE International Conference on Computer Vision*, pages 1440–1448, 2015.
- [7] Ross Girshick, Jeff Donahue, Trevor Darrel, and Jitendra Malik. Rich feature hierarchies for accurate object detection and semantic segmentation. In *IEEE Int. Conf. on Computer Vision and Pattern Recognition*, 2014.
- [8] G Gkioxari and J Malik. Finding action tubes. In *IEEE Int. Conf. on Computer Vision and Pattern Recognition*, 2015.
- [9] A Gorban, H Idrees, YG Jiang, A Roshan Zamir, I Laptev, M Shah, and R Sukthankar. Thumos challenge: Action recognition with a large number of classes, 2015.
- [10] Yonghao He, Hao Liu, Wei Sui, Shiming Xiang, and Chunhong Pan. Liris harl competition participant, 2012. Institute of Automation, Chinese Academy of Sciences, Beijing <http://liris.cnrs.fr/harl2012/results.html>.
- [11] Manan Jain, Jan Van Gemert, Hervé Jégou, Patrick Bouthemy, and Cees GM Snoek. Action localization with tubelets from motion. In *Computer Vision and Pattern Recognition (CVPR), 2014 IEEE Conference on*, pages 740–747. IEEE, 2014.
- [12] H. Jhuang, J. Gall, S. Zuffi, C. Schmid, and M. Black. Towards understanding action recognition. *Proc. Int. Conf. Computer Vision*, 2013.
- [13] Shuiwang Ji, Wei Xu, Ming Yang, and Kai Yu. 3d convolutional neural networks for human action recognition. *Pattern Analysis and Machine Intelligence, IEEE Transactions on*, 35(1):221–231, Jan 2013.
- [14] YG Jiang, J Liu, A Roshan Zamir, G Toderici, I Laptev, M Shah, and R Sukthankar. Thumos challenge: Action recognition with a large number of classes. <http://csrcv.ucf.edu/THUMOS14>, 2014.

- [15] Andrej Karpathy, George Toderici, Sanketh Shetty, Thomas Leung, Rahul Sukthankar, and Li Fei-Fei. Large-scale video classification with convolutional neural networks. In *IEEE Int. Conf. on Computer Vision and Pattern Recognition*, 2014.
- [16] A. Kläser, M. Marszałek, C. Schmid, and A. Zisserman. Human focused action localization in video. In *International Workshop on Sign, Gesture, Activity*, 2010.
- [17] Alex Krizhevsky, Ilya Sutskever, and Geoffrey E. Hinton. Imagenet classification with deep convolutional neural networks. In *Advances in Neural Information Processing Systems*, 2012.
- [18] Hildegard Kuehne, Hueihan Jhuang, Estíbaliz Garrote, Tomaso Poggio, and Thomas Serre. Hmdb: a large video database for human motion recognition. In *Computer Vision (ICCV), 2011 IEEE International Conference on*, pages 2556–2563. IEEE, 2011.
- [19] Ivan Laptev and Patrick Pérez. Retrieving actions in movies. In *Computer Vision, 2007. ICCV 2007. IEEE 11th International Conference on*, pages 1–8. IEEE, 2007.
- [20] Joseph Redmon, Santosh Divvala, Ross Girshick, and Ali Farhadi. You only look once: Unified, real-time object detection. *arXiv preprint arXiv:1506.02640*, 2015.
- [21] Shaoqing Ren, Kaiming He, Ross Girshick, and Jian Sun. Faster R-CNN: Towards real-time object detection with region proposal networks. In *Advances in Neural Information Processing Systems*, pages 91–99, 2015.
- [22] Juan C. SanMiguel and Sergio Suja. Liris harl competition participant, 2012. Video Processing and Understanding Lab, Universidad Autonoma of Madrid, Spain, <http://liris.cnrs.fr/harl2012/results.html>.
- [23] Karen Simonyan and Andrew Zisserman. Two-stream convolutional networks for action recognition in videos. In *Advances in Neural Information Processing Systems 27*, pages 568–576. Curran Associates, Inc., 2014.
- [24] Karen Simonyan and Andrew Zisserman. Very deep convolutional networks for large-scale image recognition. *arXiv preprint arXiv:1409.1556*, 2014.
- [25] Khurram Soomro, Amir Roshan Zamir, and Mubarak Shah. UCF101: A dataset of 101 human action classes from videos in the wild. Technical report, CRCV-TR-12-01, 2012.
- [26] Khurram Soomro, Haroon Idrees, and Mubarak Shah. Action localization in videos through context walk. In *Proceedings of the IEEE International Conference on Computer Vision*, 2015.
- [27] Yicong Tian, Rahul Sukthankar, and Mubarak Shah. Spatiotemporal deformable part models for action detection. In *Computer Vision and Pattern Recognition (CVPR), 2013 IEEE Conference on*, pages 2642–2649. IEEE, 2013.
- [28] J.R.R. Uijlings, K.E.A. van de Sande, T. Gevers, and A.W.M. Smeulders. Selective search for object recognition. *Int. Journal of Computer Vision*, 2013. URL <http://www.huppelen.nl/publications/selectiveSearchDraft.pdf>.

- [29] Jan C van Gemert, Mihir Jain, Ella Gati, and Cees GM Snoek. Apt: Action localization proposals from dense trajectories. In *BMVC*, volume 2, page 4, 2015.
- [30] H. Wang, A. Kläser, C. Schmid, and C. Liu. Action Recognition by Dense Trajectories. In *IEEE Int. Conf. on Computer Vision and Pattern Recognition*, 2011.
- [31] Heng Wang and Cordelia Schmid. Action Recognition with Improved Trajectories. In *Proc. Int. Conf. Computer Vision*, pages 3551–3558, 2013.
- [32] Limin Wang, Yu Qiao, and Xiaoou Tang. Video action detection with relational dynamic-poselets. In *Computer Vision–ECCV 2014*, pages 565–580. Springer, 2014.
- [33] Limin Wang, Yu Qiao, Xiaoou Tang, and Luc Van Gool. Actionness estimation using hybrid fully convolutional networks. In *CVPR*, pages 2708–2717, 2016.
- [34] Philippe Weinzaepfel, Zaid Harchaoui, and Cordelia Schmid. Learning to track for spatio-temporal action localization. In *IEEE Int. Conf. on Computer Vision and Pattern Recognition*, June 2015.
- [35] C. Wolf, J. Mille, E. Lombardi, O. Celiktutan, M. Jiu, E. Dogan, G. Eren, M. Baccouche, E. Dellandrea, C.-E. Bichot, C. Garcia, and B. Sankur. Evaluation of video activity localizations integrating quality and quantity measurements. In *Computer Vision and Image Understanding*, 127:14–30, 2014.
- [36] Christian Wolf, Julien Mille, Eric Lombardi, Oya Celiktutan, Mingyuan Jiu, Moez Baccouche, Emmanuel Dellandrea, Charles-Edmond Bichot, Christophe Garcia, and Bâijlent Sankur. The LIRIS Human activities dataset and the ICPR 2012 human activities recognition and localization competition. Technical Report RR-LIRIS-2012-004, LIRIS UMR 5205 CNRS/INSA de Lyon/Université Claude Bernard Lyon 1/Université Lumière Lyon 2/École Centrale de Lyon, March 2012. URL <http://liris.cnrs.fr/publis/?id=5498>.
- [37] Zhongwen Xu, Yi Yang, and Alexander G Hauptmann. A discriminative cnn video representation for event detection. *arXiv preprint arXiv:1411.4006*, 2014.
- [38] Serena Yeung, Olga Russakovsky, Ning Jin, Mykhaylo Andriluka, Greg Mori, and Li Fei-Fei. Every moment counts: Dense detailed labeling of actions in complex videos. *arXiv preprint arXiv:1507.05738*, 2015.
- [39] Gang Yu and Junsong Yuan. Fast action proposals for human action detection and search. In *Proceedings of the IEEE Conference on Computer Vision and Pattern Recognition*, pages 1302–1311, 2015.
- [40] C Lawrence Zitnick and Piotr Dollár. Edge boxes: Locating object proposals from edges. In *Computer Vision–ECCV 2014*, pages 391–405. Springer, 2014.